

# SMOS PAYLOAD PERFORMANCE ASSESSMENT

Martín-Neira M.<sup>(1)</sup>, Corbella I.<sup>(2)</sup>, Torres F.<sup>(2)</sup>, Cabot F.<sup>(3)</sup>, Closa J.<sup>(4)</sup>, Kainulainen J.<sup>(5)</sup>, Castro R.<sup>(6)</sup>, Barbosa J.<sup>(6)</sup>, Gutierrez A.<sup>(6)</sup>, Martín-Porqueras F.<sup>(7)</sup>, Oliva R.<sup>(7)</sup>, Anterrieu E.<sup>(8)</sup>, Brown M.<sup>(1)</sup>, McMulan K.<sup>(1)</sup>,

<sup>(1)</sup>ESA-ESTEC, Keplerlaan 1, 2200-AG Noordwijk (The Netherlands)

<sup>(2)</sup>UPC, Barcelona (Spain)

<sup>(3)</sup>CESBIO, Toulouse (France)

<sup>(4)</sup>EADS-CASA Espacio, Madrid (Spain)

<sup>(5)</sup>Aalto University, Helsinki (Finland)

<sup>(6)</sup>DEIMOS, Lisboa (Portugal)

<sup>(7)</sup>ESA-ESAC, Villanueva de la Cañada (Spain)

<sup>(8)</sup>OMP, Toulouse (France)

## ABSTRACT

The performance requirements of the SMOS payload are demanding in terms of spatial resolution, accuracy, stability and precision, all critical to fulfill its scientific objectives. For this reason a commissioning plan for MIRAS was carefully devised to verify, calibrate and characterize all instrument parameters which could have an impact on its performance. This presentation describes the most important results from the instrument commissioning phase.

*Index Terms*— SMOS, MIRAS, radiometry

## 1. INTRODUCTION

SMOS, ESA's Earth Explorer water mission with the objective of producing global maps of Soil Moisture and Ocean Salinity, was launched 2 November 2009. It carries a single payload, MIRAS, the first-ever spaceborne L-band Microwave Imaging Radiometer with Aperture Synthesis in two dimensions flown into space [1].

## 2. COMMISSIONING PHASE

Measuring the performance of SMOS in orbit was one of the main objectives of the In-Orbit Commissioning Phase of SMOS. This commissioning phase extended for 6 months comprising 4 distinct sub-phases as shown in Fig.1: 2.5 weeks of Launch and Early Orbit Phase (LEOP), 3.5 weeks (extended by 1 week) of Switch-On and Data Acquisition Phase (SODAP), 6.5 weeks of MIRAS Payload Commissioning proper, and 13.5 weeks (extended by 3 weeks) of a Pseudo-operational Phase.

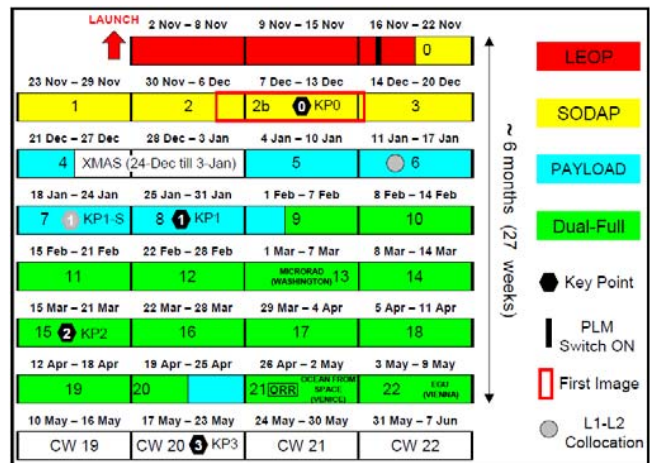


Figure 1. SMOS Payload Commissioning Plan

MIRAS was switched-on 17 November 2009. During the SODAP phase some external calibrations were executed as well as a couple of internal long calibrations. This enabled the acquisition of the first image in Week-2b.

Most of the instrument calibration tests took place during the Payload Commissioning (blue Weeks): an initial Thermal Test, where all physical temperatures were monitored, was followed by the Electrical Stability Test and the Cold Sky calibrations to acquire the Flat Target Response (FTR) of the instrument for the first time.

The pseudo-operational mode consisted of alternating weeks in dual- and full-pol modes, weekly external calibration maneuvers, and a final Electrical Stability Test in Week-20.

Table 1. SMOS Radiometric Performance Table

System Requirement Document	System Parameter	Specified Value ( $0^\circ$ = boresight, $32^\circ$ = edge of swath)	Measured Value (from ground tests)	Measured Value (in-orbit)
R-4.5.1-008	Systematic Error	1.5 K rms ( $0^\circ$ ) 2.5 K rms ( $32^\circ$ )	0.9 K rms in alias-free FoV in EMC chamber	0.33 K rms (sky) 3.2 K rms (ocean) in alias-free FoV
R-4.5.2-002-a,b	Level-1 SM Radiometric Sensitivity (1.2 s - 220 K)	3.5 K rms ( $0^\circ$ ) 5.8 K rms ( $32^\circ$ )	2.23 K rms 3.95 K rms	2.5 K rms 4.0 K rms (Antarctica)
R-4.5.3-002-a,b	Level-1 OS Radiometric Sensitivity (1.2 s - 150 K)	2.5 K rms ( $0^\circ$ ) 4.1 K rms ( $32^\circ$ )	1.88 K rms 3.32 K rms	2.0 K rms 2.5 K rms (ocean)
R-5.3.2-012	Stability (1.2 s)	4.1 K rms ( $< 32^\circ$ ) during 10 days inside EMC chamber	4.03 K rms	3.7 - 4.0 K rms (ocean, 2 weeks) in alias-free FoV
R-5.3.2-013	Stability (long integration)	0.03 K	$< 0.02$ K	$< 0.03$ K / day

### 3. RADIOMETRIC PERFORMANCE TABLE

Table 1 shows the key radiometric requirements of the SMOS mission as stated in the System Requirements Document, together with the actual values measured on ground and in orbit (last column shows the results from the commissioning phase). The instrument is compliant with all requirements with some margin, except for the systematic error over ocean (3.2 K instead of 2.5 K rms specified error), which is discussed later.

### 4. SYSTEMATIC ERROR

The systematic error in the SMOS images has two components: the offset or bias of the image (scene bias), and the ripple amplitude across the image (pixel bias). The systematic error is permanent, or changes only in long time scales, and therefore cannot be reduced by increasing the integration time or averaging.

The systematic error in SMOS images has been evaluated against the well known Cosmic Microwave Background Radiation. Fig.2 shows a typical image of the cold sky residual, that is, the difference between the SMOS cold sky image and the galactic map available from ground-based radio-astronomy surveys. The scene bias is 0.157 K and the pixel bias 0.296 K. The rms combination yields a total systematic error of 0.33 K.

The systematic error has also been assessed over ocean. The resulting ocean residuals are shown in Fig.3a and 3b for two ocean models from two independent scientific groups, for the same polarization Y. Fig.3a presents virtually no scene bias and a pixel bias of 1.35 K while Fig.4b has a scene bias of about  $-1$  K and a pixel bias near 3 K, resulting in a systematic error of 3.2 K. The worst value of the two is the one that has been included in Table 1.

Measuring the systematic error of SMOS will remain a challenge because the only target known with sufficient accuracy is the CMBR, which is outside the range of Earth surface targets (60-330 K).

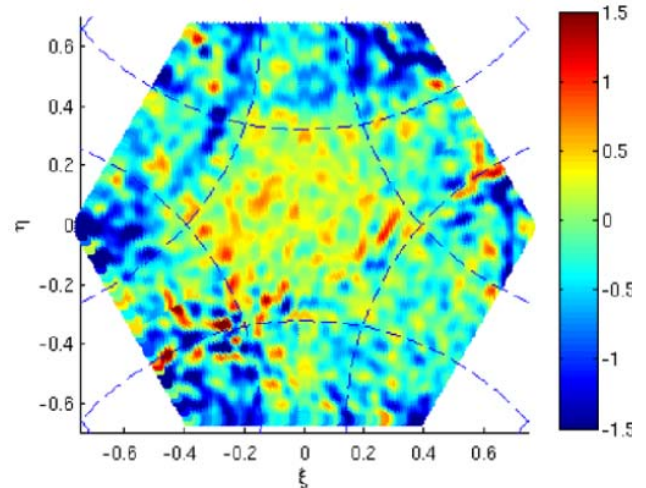


Figure 2. SMOS Cold Sky Residual

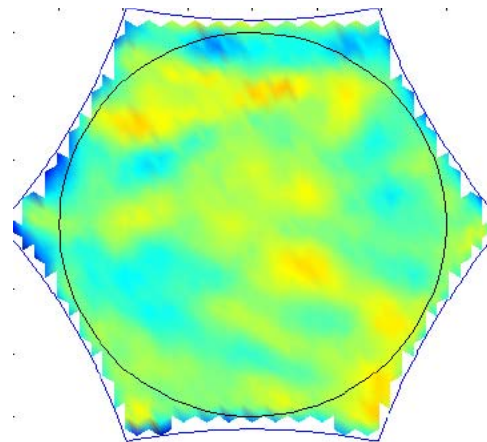


Figure 3a. SMOS Ocean Residual - 1

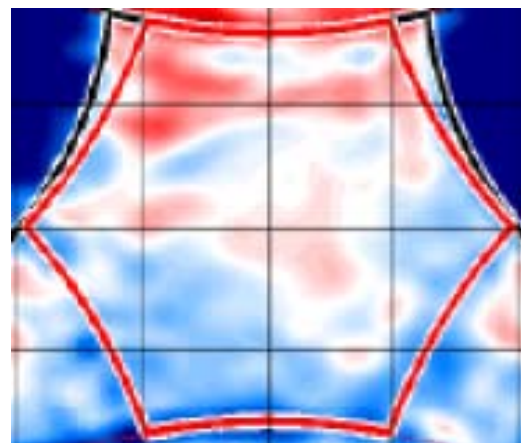


Figure 3b. SMOS Ocean Residual - 2

## 5. RADIOMETRIC SENSITIVITY

The radiometric sensitivity of SMOS is determined by the random thermal noise and can be reduced by integration or averaging. The sensitivity can be estimated by computing the temporal rms amplitude of a particular pixel in the image when observing a constant target. Pixels near boresight have better sensitivity than pixels close to the edge of the field of view because the gain of the antennas decreases away from boresight. The general expression of the sensitivity for any pixel is the following:

$$\Delta T_B(\xi, \eta) = \frac{\sqrt{3}}{2} d^2 \frac{T_A + T_R}{\sqrt{B \tau_{eff}}} \frac{\Omega_a}{t(\xi, \eta)} \sqrt{1 - \xi^2 - \eta^2} \alpha_w \sqrt{N}$$

The radiometric sensitivity of SMOS has been estimated from the cold sky and the ocean in Fig.4a and 4b respectively, where the dashed lines represent the theoretical value and the solid ones the measured temporal rms as a function of the pixel distance to boresight. The observations follow well the theoretical trend, and while they deviate by about 0.1 K the cold sky expected value, they fit theory very nicely over the ocean.

In addition, the radiometric resolution has been analysed over Antarctica. The result is shown in Fig.4c: theory and measurements fit very well with one another.

## 6. SNAPSHOT STABILITY

The snapshot stability is defined in the SMOS System Requirement Document as the rms combination of the systematic error and the radiometric sensitivity (obtained previously) evaluated over a period of 10 days. Since the latter is dependent upon the distance to boresight so is the snapshot stability. Table 2 is a summary of the snapshot stability at boresight and at the edge of the field of view.

Table 2: Snapshot Stability Table

Imaging the Ocean (over 2 weeks)		
Scene bias	-1 K	
Pixel bias	3 K	
	Boresight	At 32°
Sensitivity	2.0 K	2.5 K
Accuracy	3.7 K	4.03 K

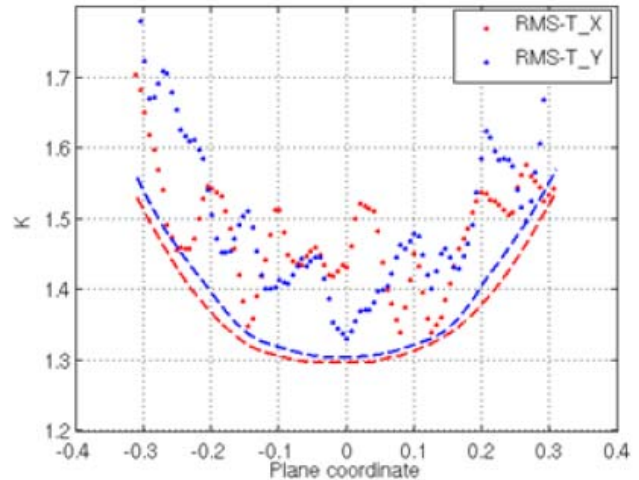


Figure 4a. Radiometric Sensitivity in Cold Sky View

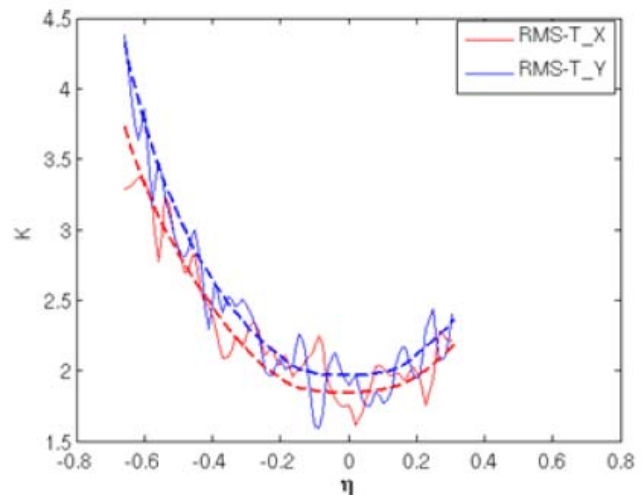


Figure 4b. Radiometric Sensitivity over Ocean

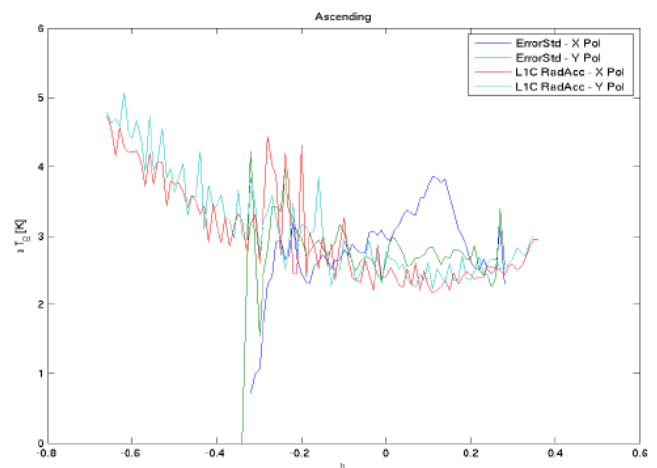


Figure 4c. Radiometric Sensitivity over Antarctica



## 7. LONG TERM STABILITY

The snapshot stability of SMOS is still under evaluation. Several parameters have been monitored throughout the commissioning phase and the stability tests performed during Weeks 4 and 20 in Fig.1 have allow analyzing their behaviour over a period of about 4 months.

The gain and offset of the LICEF receivers aboard MIRAS, as well as the correlation offsets change little over time. Moreover any drift in these parameters is tracked over time as their values are refreshed every 8 weeks through the execution of Long Calibration events.

Similarly the G-matrix, which depends on the antenna patterns and the shape of the frequency response of the receivers, has proven to be extremely stable. The G-matrix is updated only once every 6 months.

Differently to those elements above, the Noise Injection Radiometers (NIR) of MIRAS do present some fluctuation which follows what seems a seasonal trend. This is shown in Fig.5 where the antenna temperature in –the worst–horizontal polarization of the 3 NIR units and their average is plotted over time for a period of almost 4 months. As the Spring equinox is passed, the NIR units seem to start drifting. The steepest slope is 0.03 K/day.

Still today the reason for this drift which could be due to contamination from the Sun, or the Earth, through side and back lobes, but also due to the hardware, remains under investigation.

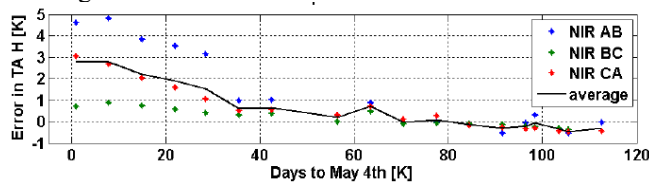


Figure 5. Apparent NIR Drift in the Boreal Spring Equinox

## 8. POINTING CALIBRATION

Geolocation biases due to launch shift and arms deployment is assessed using images over the linear coast of South-East Madagascar (Fig.6a) and a simple instrumental model (Fig.6b). Biases in roll and pitch of  $0.1406^\circ$  and  $-0.0735^\circ$  were retrieved after accumulating an extensive data set, consistent with the pre-launch error. Besides, an attempt at using the Earth horizon during external calibration maneuvers was also done (Fig.6c).

## 9. REFERENCES

[1] McMullan K., Brown M., Martín-Neira M., Rits W., Ekholm S., Marti J., Lemanczyck J., "SMOS – the Payload", IEEE Transactions on Geoscience and Remote Sensing, Vol.46, No.3, March 2008.

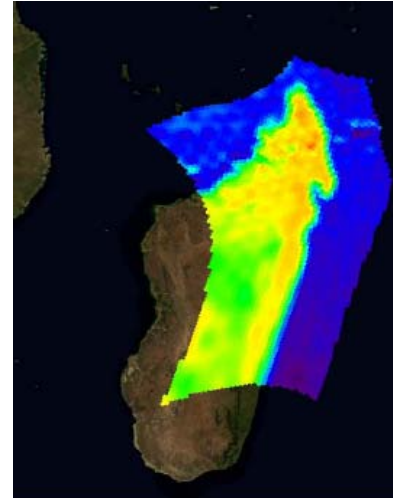


Figure 6a. Madagascar Coastline for Pointing Analysis

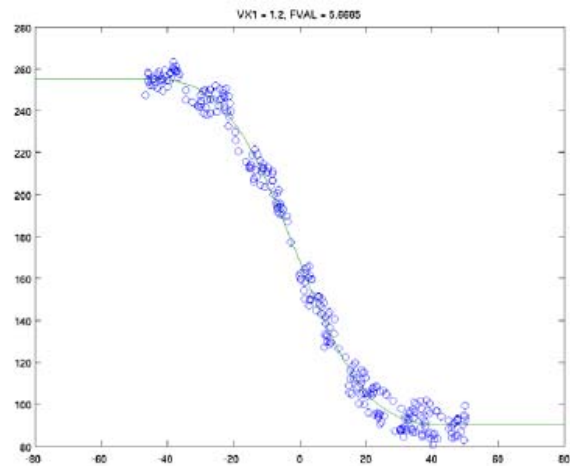


Figure 6b. Instrument Model Fit to Coastline

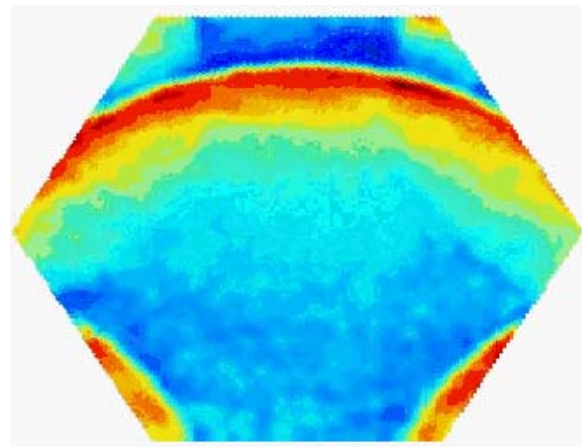


Figure 6c. Pointing Analysis with Earth Horizon